

## MerB3, an Organomercurial Lyase of *Bacillus* as an Antidote against Organomercurial Poisoning

MEI-FANG CHIEN<sup>1,2</sup>, YING-NING HO<sup>1</sup>, HUI-TZU LIN<sup>3</sup>, KUO-HSING LIN<sup>3,4</sup>,  
GINRO ENDO<sup>2</sup> and CHIEH-CHEN HUANG<sup>3\*</sup>

<sup>1</sup> Graduate School of Environmental Studies, Tohoku University, Miyagi 980–8579, Japan

<sup>2</sup> Faculty of Engineering, Tohoku Gakuin University, Miyagi 985–8537, Japan

<sup>3</sup> Department of Life Sciences, National Chung Hsing University, Taichung 420, Taiwan

<sup>4</sup> Cancer Metastasis Alert and Prevention Center, College of Chemistry, Fuzhou University, Fuzhou 350002, China

\* TEL: +886–4–2284–0416 ext. 405 FAX: +886–4–2287–4740

\* E-mail: cchuang@dragon.nchu.edu.tw

(Received: 4 March, 2019/Accepted: 4 April, 2019)

The organomercurial lyase MerB has the unique ability to cleave carbon–Hg bonds. Three *merB* genes, *merB1*, *merB2* and *merB3*, have been identified in the *Bacillus megaterium* strain MB1. To find out the similar mercury resistance gene clusters, the complete sequence of transposon TnMER1 in MB1 strain was used as a query sequence gene cluster to blast the bacterial sequences of Genbank database divisions, including 60,922 complete sequence loci and whole genome assembly database of 2,510 *Bacillus* sp. strains. The results of genome mining showed that only few *Bacillus* strains harbored TnMER1-like (three-*merB* type) mercury resistance gene clusters. However, the characterization of MerB3 protein for carbon-metal bond cleavage has not been understood. In this study, we purified MerB3 of *Bacillus megaterium* MB1 and investigated its activity *in vitro*. The protonolysis of both alkyl- and aryl-organomercurials by MerB3 were confirmed and were enhanced by thiol groups. High affinity of MerB3 to phenylmercury acetate showed the potential for using MerB3 as an antidote against organomercurial poisoning.

**Key words:** organomercurial lyase, organomercurial poisoning, MerB, genome mining

**Abbreviations:** IPTG, isopropyl β-D-1-thiogalactopyranoside; PMSF, phenylmethylsulfonyl fluoride, protease inhibitor; LB medium, Luria–Bertani medium; CVAAS, Cold vapor atomic absorption spectrometer; FPLC, fast performance liquid chromatography; PMA, phenyl mercury acetate; MMC, methyl mercury chloride; DTT, dithiothreitol; PHMB, *p*-hydroxymercuribenzoate

### 1. Introduction

Mercury is a highly mobile and reactive element that is toxic to organisms, while human activities facilitate its dissemination in the biosphere. Of all the mercury compounds, some organomercurial compounds are extremely toxic and tend to be bioaccumulated in the living organisms, such as methylmercury chloride (MMC), which has been identified as a causative agent of the Minamata disease<sup>6</sup>. Other organomercurials, such as phenylmercury acetate (PMA) and ethylmercury, were commonly used as mercury fungicide, antiseptics or disinfectants while PMA has been considered more hazardous to human than MMC<sup>10</sup>. Most of these uses have been discontinued, but small amounts of these compounds can still be found as preservatives in some medicines and threaten our daily life.

On the other hand, microbes have developed several defense systems to overcome the toxicity of mercury compounds. The most-studied mechanism is the enzymatic transformation

that degrades organomercurials to the ionic mercury, Hg<sup>2+</sup>, and subsequently reduces the Hg<sup>2+</sup> to the metallic form, Hg<sup>0</sup>. This process depends on the mercury resistance operon (*mer* operon) which consists of linked genes encode organomercury lyase (MerB), regulator (MerR), mercuric ion transporter (MerT, MerP) and mercuric ion reductase (MerA)<sup>11</sup>. Since the protonolysis of carbon–mercury (C–Hg) bonds is the first step in decomposition of organomercurials, MerB has been known as the key enzyme to mediate biological organomercurial detoxification<sup>2</sup>. The decomposition of organomercurials by MerB and subsequently mercury volatilization by MerA has been interested for applying the resistance system to the environmental mercury bioremediation and biomonitoring<sup>13,14</sup>. The most extensively characterized MerB was identified from *Escherichia coli* (plasmid R831b) and demonstrated that two highly conserved cysteines (Cys-96 and Cys-159 in R831b MerB numbering) were essential for catalytic activity. However, the MerB identified enzymes so far show low similarity and diverse substrate specificities<sup>5,8,15</sup>.

Therefore, the further studies in regarding the biochemical and structural properties of MerBs, in addition to enzymatic engineering, are required to evolve MerB for the efficient detoxification of organomercurials poisoning.

Previous study reported that in the mercury resistant bacterium, *Bacillus megaterium* MB1, three *merB* genes are identified in its transposon, Tn*MERI1*, while *merB3* gene harboring recombinant confers the broadest substrate specificity (9). Matsui *et al.*, 2016 used the PCR amplification transposon sequences of a total 65 spore-forming mercury-resistant bacteria for investigating the horizontal gene movement<sup>11</sup>). The results show that the Tn*MERI1*-like transposons can be wide horizontal dissemination across bacterial species and geographical barriers. In this study, we try to use the Tn*MERI1* transposon sequence as a query sequence gene cluster to blast and compare the bacterial sequences of Genbank database divisions and selected bacteria whole genome sequence databases for investigating the similarity of *merB* genes in mercury resistance gene cluster. In addition, we focus on the ability of the organomercury lyase MerB3 protein. In this study, MerB3 of *B. megaterium* MB1 was purified and its enzymatic properties (enzyme activity assay, substrate specificity, and kinetic analysis) were investigated. This is the first study to investigate the enzymatic properties of MerB3 in Tn*MERI1* transposon.

## 2. Materials and methods

### 2.1 Genome mining of mercury resistance gene cluster

A total of 60,922 bacterial completed sequences/loci of Genbank bacterial division (December 2018) were downloaded from National Center for Biotechnology Information (NCBI) (<https://www.ncbi.nlm.nih.gov>). The Genbank annotated whole genome sequences excluding assembly level of contig (the selected genus of *Bacillus* (2510 strains), *Paenibacillus* (161 strains), *Clostridium* (516 strains) and *Exiguobacterium* (36 strains)) were also downloaded from NCBI (at January, 2019) for constructing the selected whole genome sequence database. Homologous clusters for sequence similarity at the level of the entire gene cluster were analyzed using the MultiGeneBLAST program<sup>12</sup>). The complete sequence of transposon Tn*MERI1* from *Bacillus megaterium* strain MB1 (GenBank: LC152290.1) was used as the query sequence against the constructed database with a 30% sequence identify cut-off and 250 blastp hits mapped per query sequence. The gene clusters, which hit more than 7 genes, were selected for comparing with transposon Tn*MERI1*.

### 2.2 Bacterial strains, recombinant plasmids and culture conditions

*Escherichia coli* DH5 $\alpha$  (Invitrogen, Carlsbad, CA., USA) was used for cloning. *E. coli* Rosetta (DE3) pLysS (Novagen, Madison, WI., USA) was used for protein expression. Plasmid pET-MerB3 was constructed by PCR of *merB3* from genome DNA of *B. megaterium* MB1 by using primers merBsFrbs

(5'-GGAGGACATATGAATCAAATCATTTGAAT-3') and merB3R (5'-CACGAGTTACTTACCCTTAGAGCC-3'). The PCR product was digested with restriction enzymes *NdeI* and *XhoI*, and the *merB3*-contained *NdeI/XhoI* fragment was ligated into the expression vector pET-21b (Novagen). The MerB3 reading frame was expressed under control of the T7 promoter in the vector pET21b, and the sequence of *merB3* was confirmed by DNA sequencing. Bacteria were grown in LB medium at 37°C with agitation at 120 rpm. Ampicillin (100  $\mu$ g/ml) and chloramphenicol (35  $\mu$ g/ml) were added as needed.

### 2.3 Protein expression and purification

An overnight culture of *E. coli* Rosetta/pET-MerB3 was diluted 1 : 100 with LB medium up to 2 L and subjected to further incubation at 37°C until the absorbance at 600 nm reached 0.6. IPTG was added to the culture at a final concentration of 0.5 mM. After further incubation at 37°C for 4 h, the bacterial cells (1 L) were harvested by centrifugation (3,000 rpm, 15 min). All purification steps were performed at 4°C, and DTT-containing solutions were freshly prepared before use. The buffers used were: (A) 20 mM Tris-HCl (pH 8.0), 1 mM EDTA, 1 mM DTT, 10% glycerol; (B) 20 mM Sodium Phosphate (pH 7.5), 1 mM EDTA, 1 mM DTT, 10% glycerol; (C) 50 mM Tris-HCl (pH 7.5), 1 mM EDTA, 1 mM DTT, 200 mM NaCl. Harvested cells were suspended in buffer A with 20  $\mu$ l/10 ml PMSF. The cells were lysed using three passes through a French press at 16,000 psi. Lysates were 3 times cleared by centrifugation at 12,000 *g* for 1 h. The supernatant was passed through a 0.22  $\mu$ m filter and applied to three columns (DEAE column, sepharose column and gel filtration) for enzyme purification. The supernatant was applied to a DEAE column equilibrated with buffer A. After washing with 80 ml of buffer A, an elution program was performed with a linear gradient of 0–15 mM NaCl in the same buffer at a flow rate of 0.5 ml/min (10 ml fractions). The elution of protein was monitored by SDS-PAGE. Fractions containing organomercurial lyase were pooled. The enzyme from DEAE column was diluted to 0.1 fold by buffer B, and was applied to a Q Sepharose column equilibrated with buffer B. After washing with a bed volume of buffer B, an elution program was performed with a linear gradient of 0–0.5 M NaCl in the same buffer at a flow rate of 0.5 ml/min (10 ml fractions). The elution of protein was monitored by SDS-PAGE, and the fractions containing organomercurial lyase were pooled. The enzyme from Sepharose column was dialyzed in buffer C and concentrated to 2 ml. The enzyme was then exchanged by gel filtration into buffer C using a Superdex 75 column (GE healthcare, Piscataway, NJ., USA). The quality of purified enzyme was confirmed by 14% SDS-PAGE and N-terminal sequencing.

### 2.4 Enzyme assay and organomercurials

Organomercurial lyase activity was determined by measuring the mercury ion production from organomercurials by cold vapor atomic absorption spectrometer (CVAAS).

The assay mixture consisted of organomercurials, MerB3, and DTT was mixed and incubated at room temperature as needed. One hundred micro liter of the mixture was removed at various time intervals and analyzed for the mercury ion by CVAAS. Each experiment was done in at least triplicate. CVAAS was calibrated with mercury chloride solution. Three organomercurial compounds were used in this study; methylmercury chloride (MMC) and phenyl mercury acetate (PMA) were purchased from Wako Pure Chemical (Osaka, Japan). *p*-hydroxymercuribenzoate (PHMB) was purchased from Sigma Chemical Co. (St. Louis, Mo, USA).

### 3. Results and discussion

#### 3.1 Genome mining of TnMER11-like transposons in bacterial database

Nowadays, nucleotide sequence information was explosive growth by the development of next generation sequencing technology. Genbank is a public database of nucleotide sequences and biological annotations. There are 60,922 complete sequences/loci in the bacterial division in Genbank (BCT) (the latest file: BCT566, December 2018). After blasting entire mercury resistance gene cluster of TnMER11 transposon against BCT database, we found only *Bacillus cereus* RC607 and *Bacillus* sp. TW6 harboring three MerB encoding genes (*merB1*, *merB2*, and *merB3*) without group II intron in the mercury resistance gene cluster (Fig. 1A). The similar transposon Tn6294 in *Paenibacillus* sp. EOA1 is lack of *merB2* and *merB3* genes and the mercury resistance gene cluster in *Clostridium butyricum* is lack of MerB3, transposase, and resolvase genes (Fig. 1A). However, this process cannot hit the mercury resistance gene cluster (Tn5085) from *Exiguobacterium* sp. TC38-2b, which is harboring MerB genes (*merB1*, *merB2*, and *merB3*)<sup>3</sup>. The probable reason is incomplete sequence information in Genbank database. The public sequences of *Exiguobacterium* sp. TC38-2b are partial transposon Tn5085 encoding *tnpR* and *tnpA* genes (Y17750), partial transposase genes (Y17751, Y17752), *mer* operon (X99457) and partial *merB* (Y08064). So, we collected whole genome sequences of the genus of *Bacillus*, *Paenibacillus*, *Clostridium* and *Exiguobacterium* for constructing the selected database. After blasting, we found only four matched strains (*Bacillus cereus* #17, *B. cereus* strains B4120, B4155 and B4079) in the selected database. *Bacillus cereus* #17 (JYFW01000036) was isolated from mouse gut<sup>4</sup>. This strain #17 has 100% identity of *merB* genes (*merB1*, *merB2* and *merB3*), shorter *merP* (98% identity, 75% coverage) and *merA* genes (99% identity, 89% coverage) by comparing with TnMER11 (Fig. 1B). *Bacillus cereus* B4120, B4155 and B4079 were isolated from water, beef salad, and canned chocolate beverage, individually<sup>7</sup>. These strains have similar gene cluster harboring *merB* genes (absent of *merB1* in the strain B4079) and lack a mercuric transport protein, *merT* encoding gene (Fig. 1B). We could use this method to find out potential mercury resistance strains which harboring similar gene clusters. In addition,

this method could be used in discovering novel bacterial mercury resistant systems which contain mercury resistance gene clusters different with known ones.

Through the genome mining, we could find more similar gene clusters from different sources and different regions. The results of genome mining show that the gene clusters of three-*merB* type are very rare in bacteria (only 6 gene cluster sequence loci in ~63,000 complete sequence loci and whole genome databases of *Bacillus*, *Paenibacillus*, *Clostridium* and *Exiguobacterium*) (Fig. 1). Since the structural and biochemical characterization of MerB and MerB2 were investigated<sup>9,16,17</sup> and *E. coli* with the plasmid that harbored *merB3* of *B. megaterium* MB1 can confer a broad specificity to decompose various organomercurials<sup>5</sup>, we focused on MerB3 of *B. megaterium* MB1 and purified MerB3 protein by heterogeneous expression.

#### 3.2 Purification of MerB3

The previous study by *in vivo* experiments has reported the broad substrate specificity of MerB3. The over expression of MerB3 by IPTG induction in both pellet and soluble fraction (supernatant) of bacterial lysate was confirmed by 14% SDS-PAGE (Fig. 2A, lane P, S, T with IPTG induction). The soluble fraction was then used for purification. Our previous study corrected the original Genbank registered sequence of *merB3* gene and indicated that *merB3* is a 729 bp-frame gene and encodes a 242-amino acid polypeptide<sup>5</sup>. This open reading frame was applied to the ExPASy proteomics server (Expert Protein Analysis System: <http://au.expasy.org/>). According to the prediction on ExPASy, the molecular weight of MerB3 is 27.4 kDa, and the pI of MerB3 is 4.37. Therefore, the weak anion exchanger DEAE column suitable for purifying proteins from pH 2 to 9 was applied as the first column. Each 10 ml of elution was collected as a fraction and was analyzed by 14% SDS-PAGE. As shown in Fig. 2B, the fraction 12 of DEAE column purified products showed a major signal near 30 kDa with limited contamination proteins. Thus this fraction was chosen and applied to a strong anion exchanger, Q Sepharose column. Every 10 ml of elution was collected and analyzed by 14% SDS-PAGE. Fig. 2C shows that the fractions 14 and 15 contain large amount of protein in target size with few impurity. These two fractions were then applied to gel filtration and the purified protein was confirmed by 14% SDS-PAGE (Fig. 2D) and by N-terminal sequencing as MerB3.

#### 3.3 Enzyme assay

CVAAS was employed to measure the concentration of mercury ion in the solution by reducing the mercury ion and measuring the transmittance of mercury vapor at 253.7 nm. Since organomercurial lyase broke the carbon-mercury bond of organomercurials and yields mercury ion, CVAAS was applied to determine the activity of MerB3. Fig. 3A shows the calibration curve of CVAAS by using mercury chloride solution. MerB3, PMA and DTT were mixed in the molecular ratio of 0.01 : 1 : 2. The mixture was incubated at room

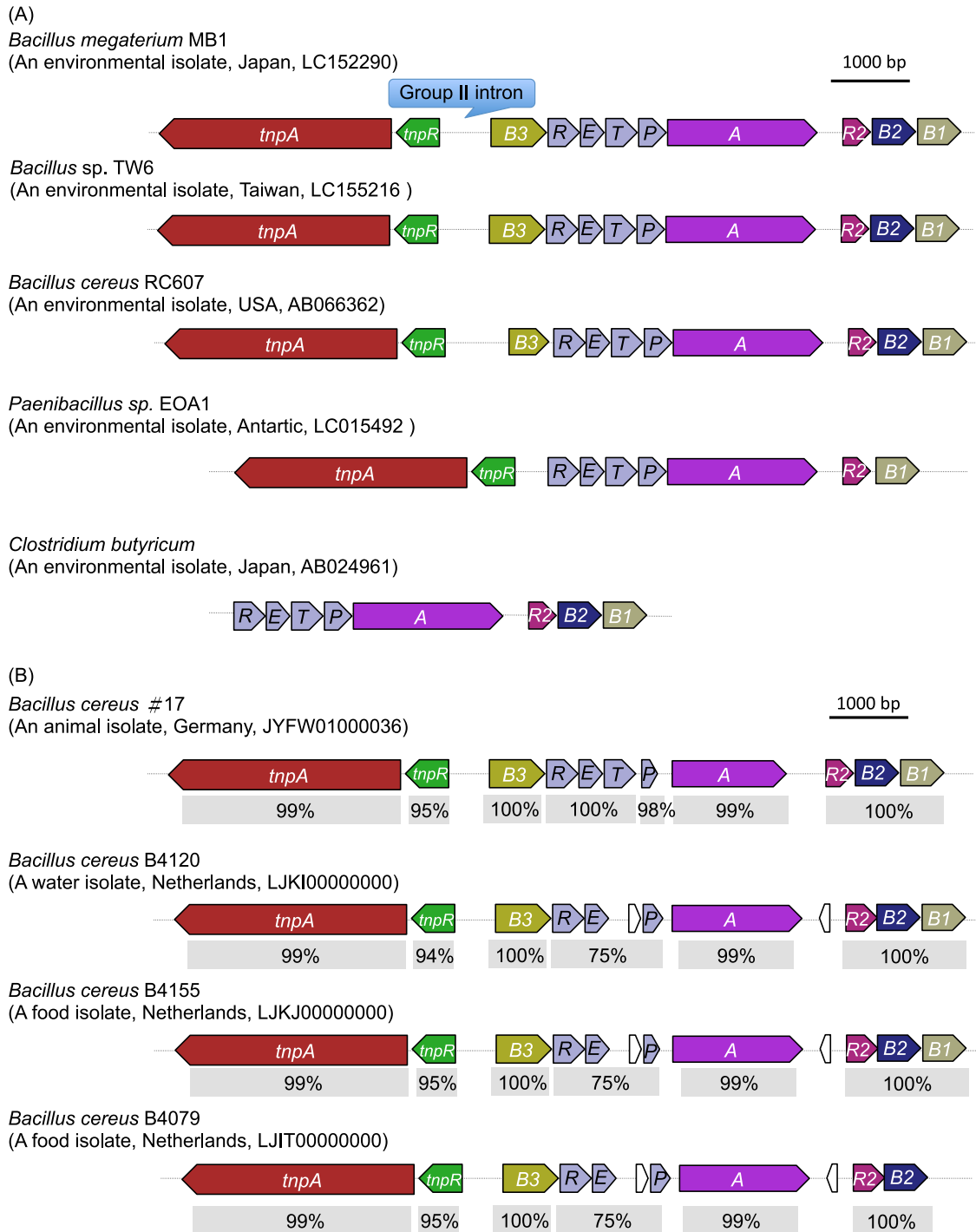


Fig. 1. The selected blasting results of *mer* gene modules among bacteria by using MultiGeneBlast. (A) Results of BCT database (Genbank: bacterial division, December 2018). (B) Results of selected database (whole genome sequences of *Bacillus*, *Paenibacillus*, *Clostridium*, and *Exiguobacterium* genus). The threshold of gene identity is 30% and the gene clusters, which hit more than 7 genes, were selected. Gray shaded boxes below genes show the regions of DNA sequence homology (the percent of identify by comparing with transposon TnMER11). Isolation sources, regions and GenBank accession numbers are listed following bacterial strains. *tnpA*: transposase; *tnpR*: resolvase; B3: organomercurial lyase *merB3*; R: mercury-responsive transcriptional regulatory protein *merR*; E: mercury resistance protein *merE*; T: mercury transport protein *merT*; P: metal binding protein *merP*; A: Mercuric reductase protein *merA*; R2: mercury-responsive transcriptional regulatory protein *merR2*; B2: organomercurial lyase *merB2*; B1: organomercurial lyase *merB1*.

temperature, and the concentration of mercury ion in the mixture was measured by CVAAS. As shown in Fig. 3, there was no mercury ion production detected from the solution contains only PMA and without MerB3, but the mercury ion production was detected from the mixture. The activity

of MerB3 to all organomercurials used in this study was also confirmed (data not shown). The result showed that the purified MerB3 has activity, and this facile spectrophotometric assay is workable on evaluating activity of MerB3.

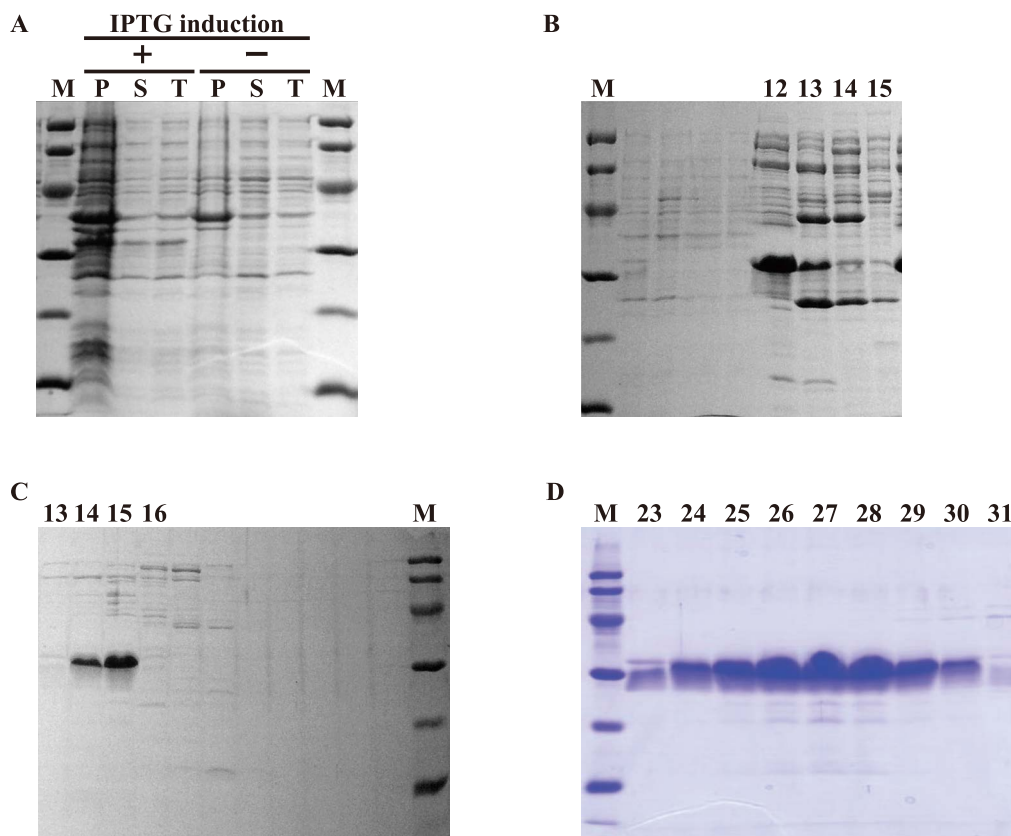


Fig. 2. Expression and purification of MerB3. (A) SDS-PAGE image of the recombinant MerB3 protein. M, protein molecular weight marker; P, pellet of cell lysate; S, supernatant of cell lysate; T, total cell lysate. (B) SDS-PAGE image of fractions from DEAE column. M: protein molecular weight marker; 12–15, the numbers of fractions. (C) SDS-PAGE image of fractions from Q-Sepharose column. M: protein molecular weight marker; 13–16, the numbers of fractions. (D) SDS-PAGE image of fraction 23 to 31 from Gel-filtration. M: protein molecular weight marker; 23–31, the numbers of fractions. The size of each band in the marker from up to bottom is 97, 66, 45, 30, 20.1, 14.4 kDa, respectively.

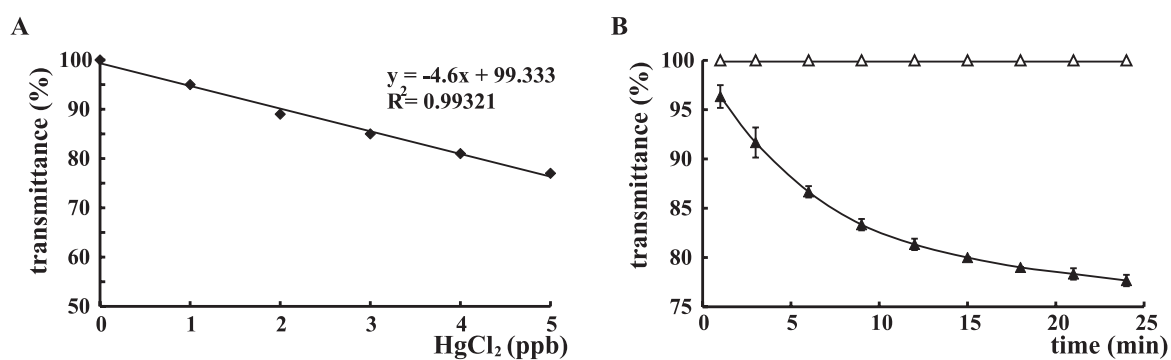


Fig. 3. Enzyme assay by CVAAS. (A) The calibration curve by using mercury chloride (black diamond) in the concentration of 0–5 ppb. X-axis: the concentration of mercury chloride; Y-axis, the transmittance of the solutions at 253.7 nm. The equation of calibration and the determination coefficient ( $R^2$ ) were shown. (B) The enzyme activity of MerB3 to PMA within 24 min. X-axis, reaction time; Y-axis, the transmittance of the reaction solutions contains PMA only (empty triangle) and PMA with MerBs (black triangle) at 253.7 nm.

### 3.4 Substrate specificity of MerB3

The substrate specificity and enzyme activity of MerB3 was then investigated. In these experiments, PMA and MMC represented as the substrate of aryl- and alkyl-organomercurials, respectively. The purified MerB2 of TnMER11 was also applied. The organomercurials, MerB enzymes and DTT were mixed in the molecular ratio of

1 : 1 : 2, and after incubating at room temperature for 6 hours, the mercury ion production was determined. As shown in Fig. 4, MerB3 catalyzed the protonolysis of the carbon-mercury bonds of both PMA and MMC, while MerB2 only performed slightly activity to PMA and almost no activity to MMC. These results show that MerB3 could perform activity to both aryl- and alkyl-organomercurials. It also showed that MerB3 performs broader substrate

specificity than MerB2 does, and it was consistent with our previous study through *in vivo* experiments<sup>5,8</sup>. Though low homology among those MerB enzymes have been showed, the phylogenetical analysis and the secondary structure predictions divided the MerB enzymes into three distinct subfamilies<sup>15</sup>. Following this grouping, MerB3 and MerB2 of MB1 belong to the same secondary structural group. However, since the sequence of *merB3* has been corrected and the quite different substrate specificity and enzyme activity of MerB2 and MerB3 are confirmed *in vivo* and *in*

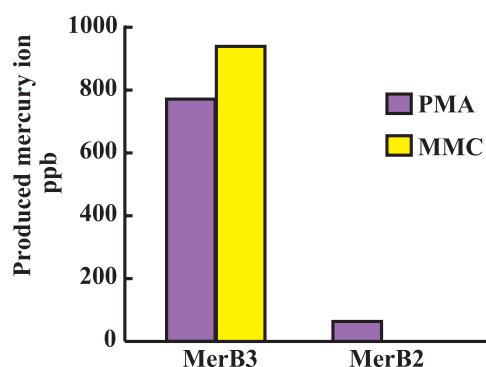


Fig. 4. The substrate specificity between MerB3 and MerB2 in *B. megaterium* MB1. Y-axis: the concentration of mercury ion production from the reaction solution.

*vitro*<sup>5</sup>) (Fig. 4), the phylogenetical analysis of MerBs need to be re-investigated.

### 3.5 Effect of thiol group on MerB3 catalyzed protonolysis

The alignment of MerB proteins identified so far has shown that the well-conserved sequences of MerB located in the central region with 3 cysteines, which the part is the most likely protein ligand for Hg<sup>15</sup>. Previous study on the most extensively characterized MerB from plasmid R831b presented that the high thiol requirement in MerB catalyzed protonolysis is due to the stuck state intermediate, that can be removed by extracellular thiol groups<sup>15</sup>. MerB3 identified from *B. megaterium* MB1 contains 242 amino acids is longer than that of MerB from R831b. And MerB3 contains other 6 cysteines in center and C-terminal other than the conserved 3 cysteines (Fig. 5A). In order to determine the effect of thiol group on MerB3 catalyzed protonolysis, organomercurials degradation experiments were performed with or without DTT addition. PMA or MMC was mixed to MerBs in the molecular ratio of 1 : 1, and the mercury ion production was determined after 6 hours incubation at room temperature. As shown in Fig. 5B, with DTT addition, both the mercury ion productions from MerB3 catalyzed PMA protonolysis and MMC protonolysis increased. It suggested the existence of the thiol group helps to remove the stuck state of MerB3. Besides, the effect of DTT addition to MMC protonolysis

**A**

MerB3 MB1	MNQMHLNLSL	KDKVLQSLGL	PEEGFEGKIR	LLSPSENSIR	LDILLFMAEG	KIVNINDLTA	60
MerB R831b	MKLAPYILEL	LTSVNRNTNGT	AD-----	LLVP-----	--ILRELAKG	RPVSRITLAG	44
consensus	M.....L	...V...G.	.....	LL.P.....	...L...A.G	...V...L..	
MerB3 MB1	TEEQIDVQSA	LQRLRELDLI	HWDQNSGDVN	VAYPFSGVPT	PHRVTLAGML	PAYSMCAIDA	120
MerB R831b	ILDW-PAERV	AAVLEQATST	EYDKD-GNI-	IGYGLTLRET	SYVFEIDRR	-LYAWCALDT	100
consensus	.....	...L.....	...D...G..N	...Y.....T	.....	...Y..CA.D.	
MerB3 MB1	LGIPSMF-TD	AVIESECAF	GEKITIDVK-	NMPPVANPDT	VVVGLTGTT-D	AADTNA--CC	175
MerB R831b	LIFPALIGRT	ARVSSHCAAT	GAPVSLTVSP	SEIQAVEPAG	MAVSLVLPQE	AADVRSFCC	160
consensus	L..P.....	A...S.CA..	G.....V..	.....P..	..V.L.....	AAD.....CC	
MerB3 MB1	DSSCESNEPT	SISTSCCPAI	QFYCSEEHQ	KANEKNSTTA	KDKLTLAEAF	EVGAAVFGGT	235
MerB R831b	HVHFFASVPT	A-----	-----EDW-	-ASKHQGLEG	LAIIVSVHEAF	GLGQEFNRHL	203
consensus	.....PT	.....	.....E.W.	.A.....	.....EAF	..G.....	
MerB3 MB1	LS--GSKGK						242
MerB R831b	LQTMSSRTP						212
consensus	L.....S...						

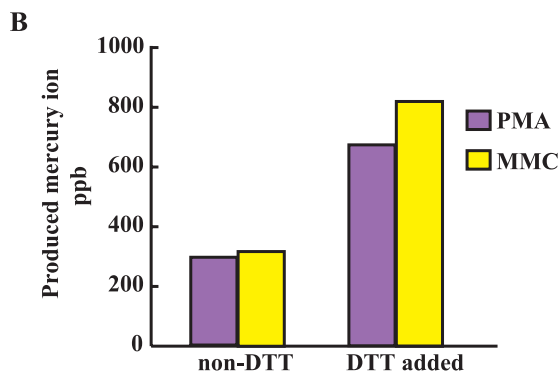


Fig. 5. (A) Alignment of amino acids between MerB3 from MB1 and MerB from R831b. The red triangles figure out the conserved 3 cysteines. (B) The effect of DTT addition on MerB3 catalyzed organomercurial degradation. Y-axis: the concentration of mercury ion production from the reaction solution.

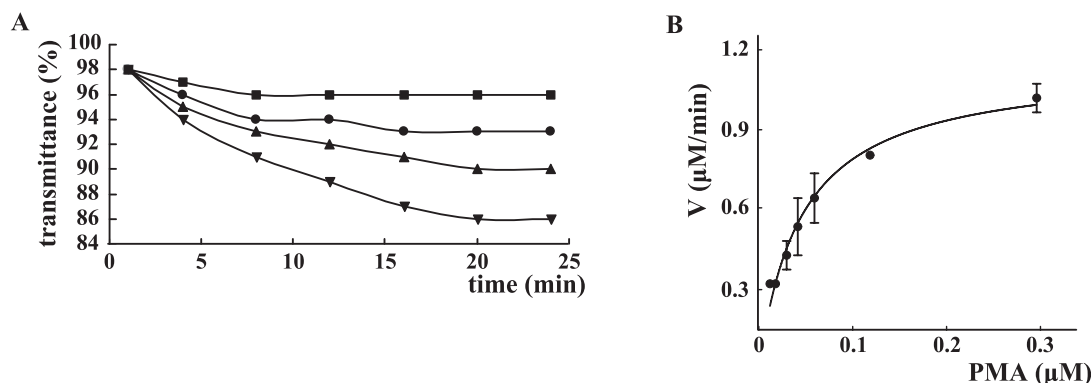


Fig. 6. Kinetic analysis of MerB3. (A) The degradation curve of MerB3 catalyzed PMA protonolysis. X-axis, reaction time (min); Y-axis, transmittance of the mercury vapor (%). The concentration of PMA is as follows. Square, 0.58  $\mu\text{M}$ ; circle, 0.87  $\mu\text{M}$ ; triangle, 1.45  $\mu\text{M}$ ; inverted triangle, 2.03  $\mu\text{M}$ . The maximal slope was reached within 5 min in all for concentration. (B) The hyperbolic distribution of MerB3 catalyzed PMA protonolysis. X-axis, the concentration of PMA reacted (mM); Y-axis: the specific reaction velocity ( $\mu\text{M}/\text{min}$ ).

was more than 30% larger than the effect to PMA protonolysis (Fig. 5B). Since the molecular of MMC is smaller than PMA, it is considered that MMC matches the active site of MerB3 looser than PMA does. Therefore, it is easier for MMC to accept the extracellular thiol groups and escape from the stuck state.

### 3.6 Kinetic analysis of MerB3

In order to further characterize the MerB3 catalyzed reaction, the mercury fungicide PMA was used as a substrate to perform the kinetic analysis. One micro gram of MerB3 was reacted to PMA in the concentration gradient varied from 0.58 to 29  $\mu\text{M}$ . The results of PMA degrading kinetic analyses at four different initial concentrations (0.58, 0.87, 1.45, 2.03  $\mu\text{M}$ ) were shown in Fig. 6A. The hyperbolic distribution of the organomercurials concentration and the reaction velocity for PMA was shown in Fig. 6B. The  $K_m$  of MerB3 to PMA was determined as  $4.5 \times 10^{-3}$  mM by applying these data to the Michaelis-Menten equation. The  $K_m$  of another MerB found from *E. coli* plasmid R831b was reported as 0.5 mM<sup>9)</sup> which was much bigger than the  $K_m$  of MerB3 from *B. megaterium* MB1. The small  $K_m$  of MerB3 from strain MB1 shows its strong substrate affinity.

In this study, MerB3 of *B. megaterium* MB1 was purified and its enzymatic properties were investigated. This study not only provides the supportive evidence regarding the substrate specificity of MerB3 but also shows that MerB3 catalyzes the protonolysis of the carbon-mercury bonds of both alkyl- and aryl-mercurials and that the existence of thiol groups enhances the MerB3 catalyzed protonolysis. Besides, the kinetic parameters of MerB3 determined by quantitative spectrophotometric assays show strong substrate affinity of MerB3. Further biochemical characterization and structural studies of MerB3 currently in progress will provide a fundamental understanding of this biotransformation of organomercurials and provide a basis for developing strategies to apply MerB3 as an antidote in detoxification of organomercurials.

### Acknowledgement

This work was supported by JSPS KAKENHI Grant-in-Aid for Exploratory Research Number 18K19042 and Grant-in-Aid for JSPS Research Fellow Number 18F18393. We thank Yu-Shin Huang and Shiao-Wei Zo (National Chung Hsing University, Taiwan) for assistance during this study.

### References

- 1) Barkay, T., S.M. Miller, and A.O. Summers. 2003. Bacterial mercury resistance from atoms to ecosystems. *FEMS Microbiol. Rev.* 27: 355–384.
- 2) Begley, T.P., A.E. Walts, and C.T. Walsh. 1986. Mechanistic studies of a protonolytic organomercurial cleaving enzyme: Bacterial organomercurial lyase. *Biochemistry.* 25: 7192–7200.
- 3) Bogdanova, E., L. Minakhin, I. Bass, A. Volodin, J.L. Hobman, and V. Nikiforov. 2001. Class II broad-spectrum mercury resistance transposons in Gram-positive bacteria from natural environments. *Res. Microbiol.* 152(5): 503–514.
- 4) Böhm, M.E., C. Huptas, V.M. Krey, and S. Scherer. 2015. Massive horizontal gene transfer, strictly vertical inheritance and ancient duplications differentially shape the evolution of *Bacillus cereus* enterotoxin operons hbl, cytK and nhe. *BMC evol. Boil.* 15(1): 246.
- 5) Chien, M-F., M. Narita, K-H. Lin, K. Matsui, C-C. Huang, and G. Endo. 2010. Organomercurials removal by heterogeneous *merB* genes harboring bacterial strains. *J. Biosci. Bioeng.* 110: 94–98.
- 6) Harada, M. 1995. Minamata disease: Methylmercury poisoning in Japan caused by environmental pollution. *Crit. Rev. Toxicol.* 25: 1–24.
- 7) Hayrapetyan, H., J. Boekhorst, A. de Jong, O.P. Kuipers, M.N.N. Groot, and T. Abee. 2016. Draft whole-genome sequences of 11 *Bacillus cereus* food isolates. *Genome Announc.* 4(3): e00485-16.
- 8) Huang, C-C., M. Narita, T. Yamagata, and G. Endo. 1999. Identification of three *merB* genes and characterization of a broad-spectrum mercury resistance module encoded by a class II transposon of *Bacillus megaterium* MB1. *Gene.* 239: 361–366.
- 9) Lafrance-Vanasse, J., M. Lefebvre, P. Di Lello, J. Sygusch, and J.G. Omichinski. 2009. Crystal structures of the organomercurial lyase MerB in its free and mercury-bound forms insights into the mechanism of methylmercury degradation. *J. Bio. Chem.* 284(2): 938–944.

- 10) Lee, C-H., R-H. Lin, S-H. Liu, and S-Y. Lin-Shiau. 1997. Distinct genotoxicity of phenylmercury acetate in human lymphocytes as compared with other mercury compounds. *Mutat. Res.* 392: 269–276.
- 11) Matsui, K., S. Yoshinami, M. Narita, M-F. Chien, L.T. Phung, S. Silver, and G. Endo. 2016. Mercury resistance transposons in *Bacilli* strains from different geographical regions. *FEMS Microbiol. Lett.* 365(5): fnw013.
- 12) Medema, M.H., E. Takano, and R. Breitling. 2013. Detecting sequence homology at the gene cluster level with MultiGeneBlast. *Mol. Biol. Evol.* 30(5): 1218–1223.
- 13) Narita, M., H. Nishizawa, H. Ishii, C-C. Huang, and G. Endo. 2003. Characterization of organomercury compounds removal by Hg-resistant *Bacillus* strains and *mer* gene cloned *Escherichia coli*. *J. Environ. Biotechnol.* 3: 43–50.
- 14) Narita, M., T. Yamagata, H. Ishii, C-C. Huang, and G. Endo. 2002. Simultaneous detection and removal of organomercurial compounds by using the genetic expression system of an organomercury lyase from the transposon TnMERII. *Appl. Microbiol. Biotechnol.* 59: 86–90.
- 15) Pitts, K.E. and A.O. Summers. 2002. The roles of thiols in the bacterial organomercurial lyase (MerB). *Biochemistry.* 41: 10287–10296.
- 16) Wahba, H.M., L. Lecoq, M. Stevenson, A. Mansour, L. Cappadocia, J. Lafrance-Vanasse, K.J. Wilkinson, J. Sygusch, D.E. Wilcox, and J.G. Omichinski. 2016. Structural and biochemical characterization of a copper-binding mutant of the organomercurial lyase MerB: Insight into the key role of the active site aspartic acid in Hg–carbon bond cleavage and metal binding specificity. *Biochemistry.* 55(7): 1070–1081.
- 17) Wahba, H.M., M.J. Stevenson, A. Mansour, J. Sygusch, D.E. Wilcox, and J.G. Omichinski. 2017. Structural and biochemical characterization of organotin and organolead compounds binding to the organomercurial lyase MerB provide new insights into its mechanism of carbon–metal bond cleavage. *J. Am. Chem. Soc.* 139(2): 910–921.